Heliyon 9 (2023) e22702

Contents lists available at ScienceDirect

Heliyon

journal homepage: www.cell.com/heliyon

The search for plausible economic mineral deposits in the central parts of Tanzania; insight from stream sediment geochemistry, multivariate statistics and geostatistics

Samuel Nunoo [a,*], Benatus Norbert Mvile [b], Mahamuda Abu [c], John Desderius Kelimenze [d]

[a] Department of Earth Science, School of Physical and Mathematical Sciences, College of Basic and Applied Science, University of Ghana, P. O. Box LG 58, Legon, Ghana
[b] Department of Physics, College of Natural and Mathematical Sciences, University of Dodoma, P. O. Box 259, Dodoma, Tanzania
[c] Department of Geological Engineering, School of Engineering, University for Development Studies, P. O. Box 1882, Nyankpala, Tamale, Tanzania
[d] Geological Survey of Tanzania (GST), P. O. Box 903, Dodoma, Tanzania

ARTICLE INFO

Keywords:
Polymetallic mineralization
Tanzania craton
Stream sediment
Geochemistry
Geostatistics

ABSTRACT

Exploration success relies heavily on the data obtained, but, significantly on the type of analytical methods deployed and the interpretation reached. A poorly analyzed data may obscure the true reflectivity of the data, and thus, compromised the decision made. A combined data processing approach of descriptive statistics, enrichment-depletion data normalization, geospatial elemental distribution, and stacked overlayed comparison of elements have been used in this study. The prime purpose was to demonstrate potential elemental anomalies, and predict areas of higher degree of confidence for subsequent exploration and mineral resource evaluation. One-hundred and sixty-six stream sediment samples from the Dodoma Region of the Tanzania Craton have been examined; to reveal potential elements or mineral commodity that warrant further exploration. Forty-three elements of target were examined, as this craton is globally known for its rich earth mineral commodity. Our result indicates an enrichment of transition metals (TMs) (Cu, Ni, Co, Cr, Mn and Zn), High Field Strength Elements (Y, Th, U, Zr, Nb, Hf, Ta and Pb), Large Ion Lithophile Elements (Ba and Rb) and Rare-Earth Elements (La and Ce), Platinum Group Element (Pd and Pt) and other metals (Au, As, Bi, W, Mo and Li).

Obtained results point to a likely poly-metallic sources and processes; as the underlain geology is marked largely by pegmatite and migmatites, and moderate proportion of fine clastic sedimentary rocks, and minor volcanic rocks mostly to the northern domain. Theoretically, the Large Ion Lithophile Elements (LILEs), Rare-Earth Elements (REEs) and Platinum Group Elements (PGEs) are associated with felsic rocks or variable stages of plutonic granitization. Although, the TMs are often associated with mafic-ultramafic rocks, the linkage of such metals with organic-rich shales been reported elsewhere. These rocks may equally contribute to the occurrence of other metals as stated in this paper. Its intriguing to note a strong positive correlation of Li with TMs, possibility of Li control by mafic minerals in pegmatite bodies. This work proposes a polymetallic enrichment controlled by the area geology. To suggest an alluvial mining potential of the above elements in the area, resource evaluation is a requirement. The geospatial maps reveal areas

* Corresponding author.
E-mail addresses: snunoo@ug.edu.gh (S. Nunoo), benimvile98@gmail.com (B.N. Mvile), mahamudaabu@gmail.com (M. Abu), jokakally@yahoo.com (J.D. Kelimenze).

https://doi.org/10.1016/j.heliyon.2023.e22702
Received 29 March 2023; Received in revised form 16 November 2023; Accepted 16 November 2023
Available online 25 November 2023

worth focusing for subsequent exploration. The adopted geostatistical methods and other approach utilized in this research are effective, indicative of handling bulk exploration data for decision and subsequent exploration.

1. Introduction

The search for geological resources such as bulk rock commodities, minerals, and elements either as metallic or non-metallic dates back centuries. The major scientific models have often been in the quest for the sources of such materials [1–8]. For example, elsewhere in the Katanga Copper belt (Democratic Republic of Congo), based on existing exploration data, various models of the source for the copper and associated elements have been proposed; syn-sedimentary [9], early to late diagenetic [10] and syn-orogenic [11]. On this same deposit, others have proposed a multiphase mineralization process [12–14]. The idea of figuring out the sources for minerals or elements, especially, the potential or the ideal host rock help to look for a similar commodity in Greenfields. For instance, the work of [7,15–17] explored for potential metallogenic source rocks. Mafic to felsic igneous rocks, and many sedimentary rocks have been proposed [4]. Others have suggested sources even outside metamorphic belt, but a proposition of metals transferred from subcrustal lithosphere [18] or even of mantle origin [19,20]. All of these models in tracing ideal source rocks for minerals or elements are based on various scientific data from both field rock-sediments exploration and laboratory analytical results.

There is no doubt that the above models mostly rely on robust data of many kinds (field, petrography, geochemistry, and isotopes). Notwithstanding, exploration data of soil, regolith, stream sediments has led to numerous exploration success story. These are cost-effective approaches in the search for most earth resources (e.g., Au, Zn, Cu and Mn). In terrains with less to no outcrop exposure, soils and stream sediments data have often given a reliable indication of likely economic mineral deposits; for example, gold search in northwest Ghana [21], and multiple deposits in parts of Tanzania, East Africa [22,23].

Promising economic mineralization potentials has thus been indicated reliably from a multidisciplinary approach that involved the use of geochemistry of soil/sediments, multivariate statistics, and geostatistics [21–23]. The objective of this research focuses on exploring for precious metals (e.g., Au, Ag and PGEs), base metals (e.g., Cu, Zn, Ni and Pb), technology and energy metals (e.g., Li, Co, U and REEs) mineralization potential within central parts of Tanzania, based on available exploratory data from stream sediment samples, largely multi-elements result obtained robustly via inductively coupled plasma mass spectrometry (ICPMS) analytical techniques, coupled with multivariate and geostatistical approaches. The obtained data is to help provide some insight into the likely

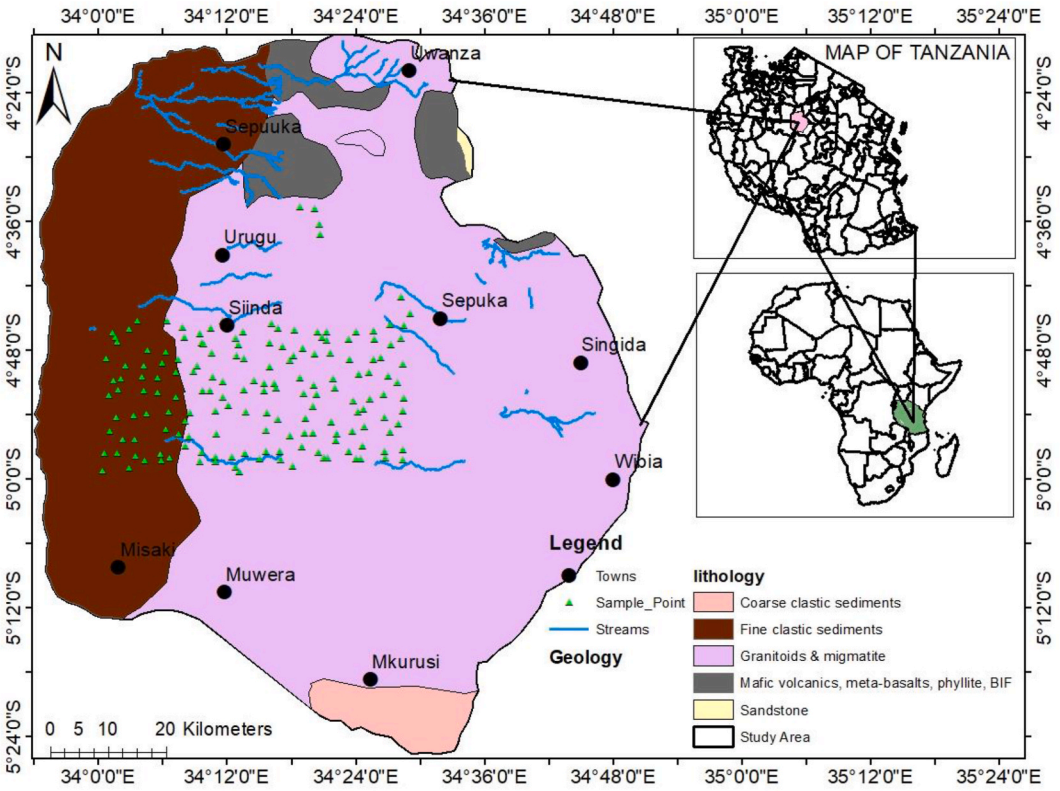

Fig. 1. Geological map of the study area with the sample locations.

potential source (s) of the promising or anomalous precious and base metals, to broaden our understanding on the long-standing debate on the potential metallogenic fertile source rocks [4–8].

2. Geological setting

The area is within the broader Tanzania Craton (TC) and is located within the central part of Tanzania [24]. The TC has a number of greenstone belts including the cluster of greenstone belts characterized by felsic gneisses and granitic rocks together with some schist [25,26]. The Siinda-Sepuka-Misaki-Singida area (Fig. 1) is within the Iramba-Sekenke greenstone belt [27,28], comprising granitoids and quartzo-felspathic gneisses, as well as stratified metavolcanic and metasedimentary rocks within the greenstone belt [29]. The older geological sequence is marked by felsic volcanic rock together with volcaniclastics, banded chert-oxide and iron formations associated with mafic volcanic rock unit [29]. The intrusive rocks are dominantly K-feldspar-rich granitoids, which occur as batholiths throughout the belt [30]. The mafic rock suite is largely foliated with gneisses and augen gneisses [29].

3. Method and materials

3.1. Field sampling and preparation

One-hundred & one samples were collected via grab sampling method from streams within the study area (Fig. 1). Sampling was done using a small clean spade, and before sampling, organic matter at depositional sites of sediments was removed (so as to prevent sample contamination, and to ensure sample), and then a sample was collected from the B-horizon (10–20 cm deep), and geographic position system (GPS) location marked. The samples were collected into calico bags were then packed in plastic bags and kept in wooden box before transported to the GST laboratory. In addition, to ensure sample condition not obliterated during transportation, sample temperature in the range of 27–31° Celsius was adhered. Preliminary sample preparation of drying and sieving to < 2 mm fraction, was carried out in the field and later transported to the Tanzania Geological Survey where they were further sieved to 75 μm at the sample preparation section of the survey department.

3.2. Laboratory analysis

Five grams of the sieved samples (of 75 micron-sized grains) from each prepared sample in sectioned 3.1 was clean-paper sealed and submitted to the Canadian Acme Laboratory for both major and trace elements analysis using the Inductively Couple Plasma Mass Spectrometry (ICP-MS) method. The platinum, palladium, and gold analysis were conducted at the Geological Laboratory of Henan, China. A thio-urea pre-concentrated of 10 g prepared from each sample after aqua regia decompositioning, produced a residue that was dissolved again in aqua regia and then the leached Au, Pd, and Pt analyzed using ICP-MS. The analysis was conducted at a detection limit 0.01 % for the oxides and 2 ppm for the trace elements. To ensure the quality of the results and the analytical procedure, duplicate and blank samples totally 25, were inserted in the samples and submitted to the laboratories for analysis. The results of the 166 samples used in the study and the 25 samples for quality check purposes, were repetitive with very minor differences. The analytical procedure followed the analytical protocols of [22,23]. The applicability of ICP-MS method covers wider geoscience-related investigation, such as measuring the extent of metal content in the soil and water samples [31].

3.3. Geostatistical and geospatial methods

A combination of statistic and multivariate statistical methods were used in the data processing to give both qualitative and quantitative representation. The suitability of multivariate statistics lies in the method's ability to reduce the complexity of compositional data while bringing out unequivocally the associations between the components of the dataset. Components of the dataset that are considered to be associated using this method have eigenvalues ≥ 1 with principal component analysis (PCA) as the extraction method. Hitherto performing this analysis, the data were transformed using the centered log-ratio (clr) method due to latent complexities associated with a compositional dataset. The statistical package for social scientist (SPSS) version 20 was used in conducting the multivariate statistics. Further details of these procedures can be found in Refs. [21–23,32,33].

Kriging interpolation method was used to carry out the geospatial analysis (*analytical tool with the Golden Surfer software, version 26.1)*. The kriging relative to other interpolation methods is suitable for characterizing spatially correlated data while making predications for locations that are sampled for one reason or the other, using results obtained from nearby sampled locations [34].

4. Results

4.1. Stream sediment trace element composition

Forty-three elements content have been measured from hundred and sixty-six stream sediment samples. These elements constitute various group such as major elements, native metals, alkali and alkali earth metals. The metals may as well be group into high- and low-field strength elements, transition metals, REEs and those of platinum group elements (PGEs), and regarded as native metals (e.g., Au) and broad categorized chalcophiles (e.g., Ag, Bi and As). Using the prime purpose of this paper, to identify the potential elemental association with initial measured concentrations that may reveal untapped mineralization zone. Dealing with multi-element

geochemical data, especially in exploration should be governed by an approach that help in revealing anomalies for further prospecting. Thirty-four elements of interest have been considered for descriptive statistics (Table 1). Maximum values based on descriptive statistics are normalized using standards from Ref. [35]. The reason is to show elements with higher or anomalous values. The enrichment-depletion normalization plot shows element either above or below the threshold line (Fig. 2). Out of the 34 elements, 26 are above the threshold, and thus considered enriched relative to those below the defined line (Fig. 2). The 26 elements that show enrichment per the adopted standard are placed into transition metals (Cu, Ni, Co, Cr, Mn and Zn), High Field Strength elements (Y, Th, U, Zr, Nb, Hf, Ta and Pb), Large Ion Lithophile (Ba and Rb) and Rare-Earth elements (La and Ce), platinum group element (i.e., PGEs, e.g., Pd and Pt) and other metals (Au, As, Bi, W, Mo and Li). The essence of these elements or metals cannot be overemphasized, as these are major drivers in the clean energy technology and industrialization. For instance, Au and Li continue to form part of super-computer fabrication and batteries respectively.

The element groupings have been presented as sub-sections under result, distribution pattern maps of their occurrences are shown, and their correlation metrics tabulated. There are mostly based on the geostatistical treatment of the data. Aspects on correlation plots, principal component and factor analyses have been included for detailed treatment of the obtained data. Such results offer insight possible geological controls on the nature of mineralization, especially where positive correlation exists and or different attribution of an observed pattern [21].

4.2. Correlation matrix and stack bivariate plot

Twenty-six elements with their respective average and standard deviation (Table 1) represent the potential mineralization target shown largely by the normalization plot (Fig. 2). To measure the degree of relationship that exist among these promising elements, Pearson correlation matrix (Table 2) and multiple stacked bivariate plots (Fig. 3) have been presented. In this paper, the concern centers on associations that show positive correlation. The strength of correlation considered here is the moderate (values from 0.60 to 0.70), higher (0.71–0.79) and the strongly (values $>$ 0.79) correlation. Elements with significant correlation values are highlighted in red in Table 2, these do show a general positive correlation (implying a concomitant increase of one element as the other increases). An important observation is often positive correlation of moderate through higher to strongly correlation of elements belonging to the same group. For example, Pb exhibits such degree of correlation with Hf, Y, Ce, U, La and Th (Table 2); as largely HFSE. Most transition metals as well show similar correlation, for instance, transition metals of Ni, Cu, Co and Zn (Table 2). Another significant observation is

Table 1
Descriptive statistical summary of elements (in ppm) considered in this study.

	N	Range	Minimum	Maximum	Mean	Std. Dev.	Variance	Skewness	Kurtosis
Mo	166	3.90	0.20	4.10	0.88	0.52	0.28	2.86	12.44
Cu	166	31.40	1.50	32.90	7.08	4.50	20.28	2.24	8.45
Pb	166	296.70	5.30	302.00	31.67	24.44	597.30	8.37	91.39
Zn	166	184.00	3.00	187.00	25.88	17.56	308.37	5.20	43.61
Ag	166	0.30	0.00	0.30	0.01	0.04	0.00	4.27	20.30
Ni	166	56.70	1.90	58.60	10.74	7.87	61.92	2.74	11.96
Co	166	21.90	1.10	23.00	6.34	3.23	10.44	1.12	3.37
Mn	166	2899.00	66.00	2965.00	465.49	304.62	92790.55	4.05	28.16
As	166	4.00	0.00	4.00	0.81	1.02	1.04	0.94	−0.13
U	166	43.80	0.60	44.40	5.67	4.46	19.88	4.62	34.82
Pd	166	1.69	0.09	1.77	0.33	0.20	0.04	4.23	24.68
Pt	166	1.36	0.21	1.56	0.37	0.18	0.03	4.01	19.62
Au	166	4.08	0.26	4.34	0.84	0.58	0.34	3.54	16.83
Th	166	1103.50	2.50	1106.00	41.48	89.11	7940.87	10.59	125.22
Sr	166	323.00	19.00	342.00	129.73	69.60	4844.61	0.70	−0.14
Cd	166	0.40	0.00	0.40	0.04	0.08	0.01	2.21	4.51
Sb	166	0.20	0.00	0.20	0.01	0.03	0.00	4.31	19.57
Bi	166	0.50	0.00	0.50	0.11	0.11	0.01	0.73	0.08
V	166	94.00	0.00	94.00	34.35	17.14	293.90	0.65	0.75
La	166	1997.50	3.50	2001.00	83.78	188.87	35671.87	8.18	74.42
Cr	166	125.00	15.00	140.00	39.42	20.68	427.65	1.84	4.58
Ba	166	1533.00	86.00	1619.00	621.55	272.04	74008.32	0.53	0.89
W	166	5.10	0.10	5.20	0.96	0.63	0.39	2.93	13.74
Zr	166	1247.00	21.50	1268.50	248.51	167.66	28110.69	2.52	10.61
Ce	166	1994.00	7.00	2001.00	162.84	245.66	60348.98	5.97	40.02
Sn	166	4.40	0.40	4.80	1.88	0.93	0.86	0.94	0.64
Y	166	240.60	1.90	242.50	21.76	20.11	404.23	8.26	88.71
Nb	166	216.20	3.90	220.10	28.88	23.31	543.31	4.57	30.03
Ta	166	27.80	0.00	27.80	2.29	3.06	9.38	5.58	36.56
Be	166	3.00	0.00	3.00	0.93	0.90	0.82	0.44	−1.00
Sc	166	12.00	0.00	12.00	4.18	2.22	4.94	0.53	0.38
Li	166	32.50	2.20	34.70	12.32	6.94	48.18	0.89	0.36
Rb	166	351.70	21.70	373.40	152.31	66.73	4452.51	0.82	1.23
Hf	166	31.60	.60	32.20	7.49	5.28	27.86	2.16	6.64

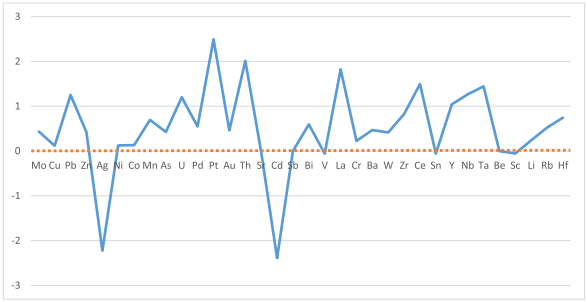

Fig. 2. Enrichment – depletion normalization (log normalized) plot based on the measured maximum value of elements in Table 1 (Normalization values from Ref. [35]).

no form of correlation between As and Au (Table 2), and these two as well are not correlated with any of the target elements in Table 2.

In Fig. 3, the graphical display of the extent of the positive correlation among element and likely group is demonstrated. For instance, the transition metals show positive correlation pattern among themselves (Fig. 3a) and other potential metals of W and Li (Fig. 3c). But in Fig. 3c, the nature of the trend between Ni and W seems to be controlled by an additional factor. Table 3 shows moderate correlation between Ni and W, and the graphical display (Fig. 3c) partially show Ni increasing even at a nearly constant value of tungsten (W). Tungsten shows similar trend when plot against thorium (Fig. 3f). The correlation trends among the HFSE (Fig. 3b and c) and REEs (Fig. 3d and e) are expected perfect or strongly correlation. However, the strongly correlation of Zn and Mn with the HFSE and some REEs indicate how these groups likely control the occurrence of the mentioned metals (i.e., Zn and Mn). A need to establish elemental linkage may be ideal to reveal those likely to act as pathfinders to other metals; dendrograms are derived under multivariate statistical analysis in sub section 4.2.

4.3. Multivariate statistical analysis

The multivariate statistical method of factor analysis (FA) and principal component (PC) extraction approach are used in this paper. In the grouping of the components, eigenvalue loadings of 0.5 are considered significant for a particular PC, are presented in Table 3. The FA accounted for 80.924 % of the total variance of the analysis (Table 3), representing 6 principal components (Table 4) deduced from the scree plot (Fig. 4), where the number of eigenvalues above 1 (Fig. 4) is the number of PCs. PC 1 accounts for 34.348 % of the total variance (80.539 %) with Pb, Zn, Mn, U, Th, La, Zr, Ce, Y, Nb, Ta and Hf (Table 4). PC 2 accounts for 20.486 % of the total variance with Mo, Cu, Ni, Co, As, Bi, Cr, W and Li, with PC 3 accounting for 8.660 % with elements of Pt and Pd. Principal components of 4, 5, and 6 account for 7.731 %, 5.557 % and 4.142 % with elements of Rb and Ba, Ta, and Au respectively. The FA and PC with their associated elemental association are mostly controlled by factors largely dependent on the regional to localized geology, and mineralization processes (e.g., mineralized source rocks, hydrothermal to metasomatic alteration and sedimentological enrichment processes) [36–38].

Another important data analysis is the cluster analysis (Fig. 5a and b), as variables and cases based on their degree of similarities, and or associations control by an underlying geological process, are revealed. For example, in Fig. 5a, placing the phenon line at 20 indicate 3 major elemental associations. Cluster 1 constitutes association of Pb, Zn, Mn, U, Th, La, Zr, Ce, Y, Nb, Ta, Hf, Ba and Rb (Fig. 5a). Cluster 2 contains Mo, Cu, Ni, Co, As, Bi, Cr, W and Li, and cluster 3 with association of Pt, Pd and Au. Cluster 1 represent a combination of PC 1 and PC 4, cluster 2 reflects PC 2, and cluster 3 containing a merge of PC 3 and PC 6. The PC 5 element of Ta is of a better factor loading in PC 1 (Table 4).

4.4. Spatial distribution of elements

Having established element that show some enrichment relative to their average crustal abundances. The crucial aspect in exploration is such element occurrences or spatial distribution within the considered geological terrane.

4.4.1. Transitional metals

The considered transition metals include Ni, Cu, Cr and Co, Zn and Mn.

4.4.2. High field strength elements

High Field Strength Elements considered include Y, Zr, Nb, U, Ta, Th, Pb and Hf.

4.4.3. Large ion lithophile elements (LILE) and REEs

LILE and REEs plotted are respectively Rb and Ba, and La and Ce.

4.4.4. PGEs and other metals

The platinum Group Element (PGE) plotted in Pt and Pd and other elements include Li, Bi, Au, As, Mo and W).

Table 2
Pearson correlation matrix of the data set (values in red are those considered significant in this paper).

	Mo	Cu	Pb	Zn	Ni	Co	Mn	As	U	Pd	Pt	Au	Th	Bi	La	Cr	Ba	W	Zr	Ce	Y	Nb	Ta	Li	Rb	Hf
Mo	1.00																									
Cu	0.52	1.00																								
Pb	0.00	−0.03	1.00																							
Zn	0.23	0.31	**0.80**	1.00																						
Ni	0.52	**0.94**	−0.08	0.24	1.00																					
Co	0.34	**0.83**	0.11	0.37	**0.81**	1.00																				
Mn	−0.06	0.03	**0.76**	**0.83**	−0.06	0.26	1.00																			
As	0.38	0.45	−0.05	0.15	0.44	0.34	−0.07	1.00																		
U	0.02	−0.03	**0.85**	**0.79**	−0.09	0.11	**0.79**	0.01	1.00																	
Pd	0.01	0.20	−0.09	−0.06	0.15	0.19	−0.07	0.19	−0.08	1.00																
Pt	−0.02	0.10	−0.01	−0.06	0.04	0.16	−0.04	0.17	−0.02	**0.77**	1.00															
Au	−0.11	−0.03	−0.06	−0.07	−0.05	−0.04	−0.08	−0.05	−0.07	0.21	0.14	1.00														
Th	0.02	−0.05	**0.95**	**0.81**	−0.10	0.04	**0.77**	−0.08	**0.83**	−0.07	−0.03	−0.03	1.00													
Bi	0.28	0.40	−0.04	0.23	0.41	0.35	0.08	0.10	0.06	0.02	−0.12	−0.13	−0.04	1.00												
La	0.03	−0.04	**0.88**	**0.73**	−0.09	0.05	**0.72**	−0.07	**0.80**	−0.07	−0.04	−0.02	**0.92**	−0.03	1.00											
Cr	0.67	0.47	−0.04	0.15	0.54	0.27	−0.09	0.21	−0.10	−0.02	−0.10	−0.11	0.09	0.21	0.06	1.00										
Ba	−0.36	−0.15	0.29	0.23	−0.19	0.11	0.45	−0.07	0.38	−0.06	0.01	−0.02	0.16	0.09	0.28	−0.55	1.00									
W	0.47	0.59	0.01	0.26	0.64	0.46	0.07	0.26	0.04	0.01	−0.15	−0.10	0.04	0.55	0.11	0.48	−0.07	1.00								
Zr	0.05	0.02	0.52	0.62	−0.05	0.13	**0.71**	0.05	**0.75**	−0.04	0.02	−0.12	0.47	0.13	0.44	−0.22	0.52	0.05	1.00							
Ce	0.02	−0.04	**0.78**	0.67	−0.10	0.05	0.69	−0.06	**0.78**	−0.06	−0.02	−0.02	**0.80**	−0.04	**0.95**	−0.03	0.39	0.13	0.51	1.00						
Y	0.05	0.03	**0.95**	**0.85**	−0.02	0.16	**0.80**	−0.04	**0.90**	−0.10	−0.04	−0.07	**0.95**	0.05	**0.88**	0.04	0.26	0.09	0.61	**0.79**	1.00					
Nb	0.26	0.11	0.46	0.53	0.12	0.10	0.46	0.03	0.55	−0.14	−0.13	−0.11	0.47	0.23	0.54	0.14	0.08	0.49	0.41	0.59	0.54	1.00				
Ta	0.06	−0.06	0.45	0.41	−0.04	−0.02	0.43	−0.07	0.53	−0.14	−0.13	−0.09	0.47	0.12	0.59	0.05	0.15	0.38	0.33	0.63	0.51	**0.94**	1.00			
Li	0.48	**0.72**	0.00	0.32	**0.75**	0.67	0.03	0.46	0.11	0.02	−0.07	−0.05	−0.04	0.55	0.02	0.34	−0.01	0.59	0.06	0.03	0.07	0.24	0.09	1.00		
Rb	−0.24	−0.23	0.32	0.15	−0.24	−0.09	0.28	−0.08	0.43	−0.16	−0.08	−0.08	0.17	0.01	0.25	−0.46	**0.51**	−0.07	0.35	0.37	0.26	0.45	0.53	0.01	1.00	
Hf	0.00	−0.02	0.60	0.64	−0.08	0.12	0.73	0.02	**0.80**	−0.01	0.06	−0.12	0.54	0.07	0.50	−0.24	0.53	0.02	**0.98**	0.56	0.67	0.43	0.37	0.02	0.39	1.00

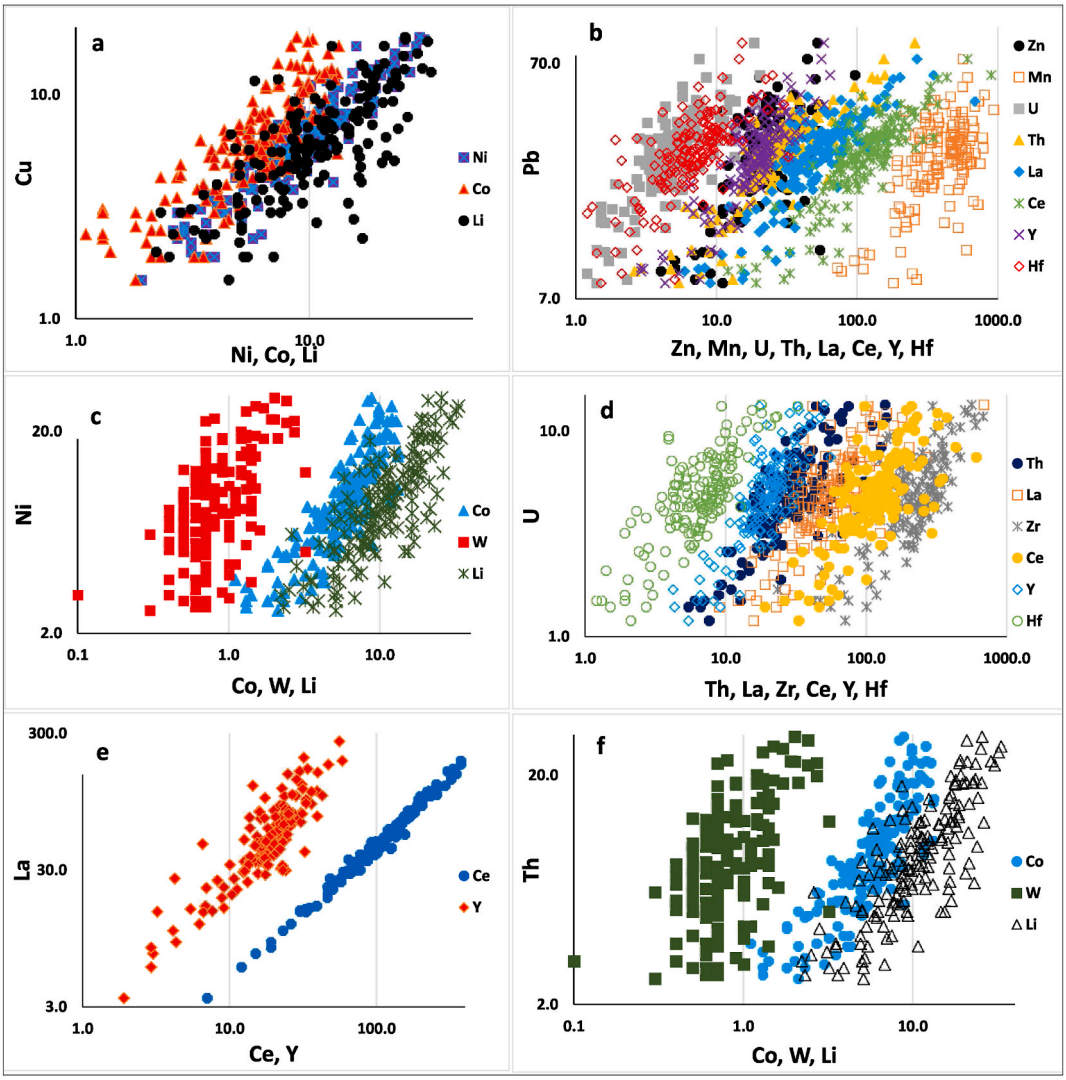

Fig. 3. Multi-stacked plots of Cu, Pb, Ni, U, La and Th; each element against several element that show positive correlation. (a) Cu against Ni, Co and Li (b) Pb against Zn, Mu, U, Th, La, Ce, Y and Hf (c) Ni against Co, W and Li (d) U against Th, La, Zr, Ce, Y and Hf (e) La against Ce and Y (F) Th against Co, W and Li.

4.5. Overlay of elements

The geospatial map superimposed on each other reveals a quick overlay to visualized similar trends, especially exemplified by the overlays of Co–Cu–Ni and Cr, and the other on Nb and Ta. The latter reveals the occurrence of Nb and Ta at the central part of the area.

5. Discussion

5.1. Implication of observed trend/pattern in exploration

Predictions of metal anomalies are often done to focus on target promising to yield economic or commercial resources [22,23]. Exploration cost largely increases with gathering of various data, and each stage should either indicate a need to continue or a reason to abandon the project. The results presented, especially, the normalization data revealed element either enriched or depleted (Fig. 2), whiles a combination from the correlation data and plots (Table 2 and Fig. 3), and the geospatial distribution revealed elements of similar trend, pattern or belong to a given cluster or group (e.g., Fig. 5). For instance, the transition metals of Ni, Cu and Co show positive correlation (Table 2 and Fig. 3a) but together with Cr (Fig. 6) show potential anomaly largely at the NE section of the area, although moderate anomalies do occur at the SW areas, besides a minor pocket occurrence. Such a reflection makes a concomitant target exploration of Ni–Co–Cu and the NE segment of the terrane a first priority should there be a follow-up exploration. The trend of

Table 3
Eigenvalues loadings for the principal components and their cumulative percentage of variance.

Component	Initial Eigenvalues			Extraction Sums of Squared Loadings		
	Total	% of Variance	Cumulative %	Total	% of Variance	Cumulative %
1	8.931	34.348	34.348	8.931	34.348	34.348
2	5.326	20.486	54.835	5.326	20.486	54.835
3	2.252	8.660	63.495	2.252	8.660	63.495
4	2.010	7.731	71.226	2.010	7.731	71.226
5	1.445	5.557	76.782	1.445	5.557	76.782
6	1.077	4.142	80.924	1.077	4.142	80.924
7	.893	3.433	84.357			
8	.819	3.151	87.508			
9	.629	2.419	89.928			
10	.511	1.965	91.892			
11	.462	1.775	93.668			
12	.282	1.086	94.754			
13	.251	.966	95.719			
14	.239	.921	96.641			
15	.209	.804	97.445			
16	.186	.717	98.161			
17	.137	.526	98.688			
18	.126	.484	99.172			
19	.064	.247	99.418			
20	.048	.184	99.602			
21	.033	.129	99.731			
22	.024	.093	99.824			
23	.023	.088	99.912			
24	.010	.040	99.953			
25	.007	.026	99.979			
26	.006	.021	100.000			

Table 4
Obtained components from the factor analysis.

	Component					
	1	2	3	4	5	6
Mo_ppm	.070	**.700**	−.204	−.188	.008	−.367
Cu_ppm	.059	**.906**	.210	.013	−.075	.122
Pb_ppm	**.894**	−.114	.016	−.263	−.094	.092
Zn_ppm	**.869**	.258	.064	−.140	−.198	.034
Ni_ppm	.000	**.931**	.113	.044	−.060	.131
Co_ppm	.196	**.748**	.366	.111	−.139	.232
Mn_ppm	**.871**	−.066	.137	−.016	−.196	.050
As_ppm	−.001	**.520**	.266	.013	.029	−.296
U_ppm	**.934**	−.091	.077	−.026	−.056	−.064
Pd_ppb_	−.107	.150	**.686**	−.290	.486	−.092
Pt_ppb_	−.061	.023	**.726**	−.293	.451	−.201
Au_ppb_	−.105	−.092	.235	−.213	.260	**.596**
Th_ppm	**.878**	−.096	−.073	−.406	−.075	.091
Bi_ppm	.123	**.535**	−.063	.398	−.025	.084
La_ppm	**.882**	−.082	−.106	−.300	.074	.150
Cr_ppm	−.032	**.662**	−.391	−.445	−.028	−.148
Ba_ppm	.424	−.292	.383	**.562**	−.106	.177
W_ppm	.197	**.741**	−.257	.202	.235	.076
Zr_ppm	**.740**	−.070	.284	.284	−.183	−.331
Ce_ppm	**.868**	−.103	−.063	−.135	.156	.108
Y_ppm	**.935**	−.028	−.015	−.236	−.101	.046
Nb_ppm	**.681**	.198	−.380	.191	.479	−.104
Ta_ppm	**.652**	.014	−.401	.188	**.563**	−.021
Li_ppm	.144	**.810**	.050	.270	−.030	.156
Rb_ppm	.432	−.307	−.018	**.579**	.320	.020
Hf_ppm	**.784**	−.118	.295	.231	−.145	−.305

the transition metals differs significantly from the correlative assemblage and the distribution pattern observed for high field strength elements (HFSE) in Fig. 7. For example, the HFSE, especially, Ta, Nb, Zr, Pb, Hf, Th, U and Y exhibits positive correlation trend (Fig. 3b and d), but with a unique pattern; as the distribution anomalies is pronounced in the central domain of the explored terrane. For exploration purposes, the focus on HFSE occurrence merits the central part of the concession, as differing to transition metals to the NE.

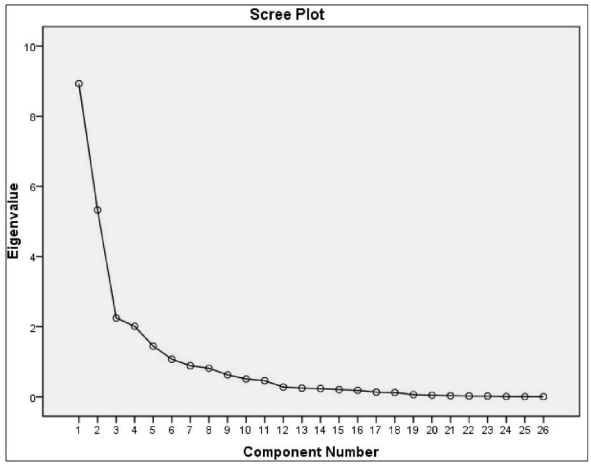

Fig. 4. The scree plot defining the number of eigenvalues above 1 accounting for a factor loading of 80.924 % total variance, and represent 6 principal components.

Furthermore, in Fig. 8, the large Ion Lithophile elements of Rb and Ba show a broader anomalous distribution, but similar trend that differs from La and Ce of REEs. The later trend (for La and Ce in Fig. 8) exhibits a petal-like shape of anomalous concentration from the near-central diminishing towards the north. A poorly observed pocket, though lateral-like pattern of La and Ce occur to the east of the area. Such trends as observed for La and Ce become tricky to extend exploration, unless re-sampling and further analysis is done to warrant the need to widen exploration with robust technique, which is often costly.

Other metals (PGEs, Bi, Li, Au and As), equally offer correlative assemblage (e.g., positive correlation between Li with Cu, Ni, Co and W; Fig. 3c and f) and a unique pattern, that suggest where to channel exploration resources should there be a follow-up campaign. The PGE of Pt and Pd are positively correlated (Table 2), but their unique distribution as anomaly (Fig. 9) shows along the SE corner of the terrane, possibly indicating the likely area to target. However, the possibility to explore areas to the immediate east of the assessed area could be a promising idea. This rational is based on the spreading pattern that indicate PGE rich areas to the east. Significantly, Li and Bi anomalies are widely spread (Fig. 9), except few areas in the central portion of the terrane with concentrations less than 0.05 ppm. These metals, especially, Li in recent times has rapidly gain a new focus, due to its effective utilization in Li-technology of the automobile industry and Li-powered batteries. The Li-occurrence, much requires further assessment if a huge potential of alluvial Li in sediments exist, possible one like ancient salars in Latin-America [39–41] or other form of alluvial occurrences though different commodity (i.e., gold) in the Paleoproterozoic terrane of Ghana [42–46]. An unexpected pattern occurs between Au and As (Fig. 9), as the later is well known for its affinity to gold [47,48], thus could display an anomalous trend similar to Au; but differing pattern was observed. However, the style of Au distribution at the NE part of the terrane (Fig. 9) appears similar to those observed for the transition metals (Fig. 6), Mo and W (Fig. 9), all with reference to the NE part of the area. This manner of geospatial distribution could suggest, a possible exploration of such elements or metal together, although caution should be taken, where considerable variable distribution pattern occurs. The layered representation (Fig. 10) offers a quick view of stacked layer of element distribution, and a display of similar pattern easily observable. The exploration of element with similar distribution pattern was basically established via the Pearson correlation matrix (Table 2) and the multi-stacked bivariate plots (Fig. 3). The geostatistical component of these elemental relationship has been expanded in section 5.2.

5.2. *Geostatistical significance and potential sources of metals*

The utilization of geostatistical approach keeps emerging great in various aspect of geoscience from mineral exploration to predictive elemental maps [21,22], sedimentological studies [49] among other areas of error check and quality control of assay data [50,51]. However, the prime focus or purpose of each data should be identified and the desired method deployed. The applied methods (e.g., Pearson correlation matrix, factor analysis (FA), principal component (PC) and dendrogram) used in this research are to allow reveal potential economic minerals among multiple elements being considered. The FA accounted for 80.924 % of the total variance of the analysis (Table 3), which translates into 3 cluster groups (Fig. 5) containing elements from the 6 PCs (Table 4). These elements are part of those evaluated as enriched (Fig. 2) per normalization using the standard of [35]. The 3 cluster groups, correlation details (Table 2 and Fig. 3), FA and PC shows elemental linkages prone to underlying geological processes such as weathering and metasomatism releasing these minerals or metals [38,52]. Processes of rock-water interaction is geological process that as well get elements released, and likely absorbed of element unto grains or sediments. The question still remains, the possible geological control mechanism, especially, source rocks that may have weathered to release the cluster groups established in this research. Cluster 1 constitutes association of Pb, Zn, Mn, U, Th, La, Zr, Ce, Y, Nb, Ta, Hf, Ba and Rb (Fig. 5a). Cluster 2 contains Mo, Cu, Ni, Co, As, Bi, Cr, W and Li, and cluster 3 with association of Pt, Pd and Au.

Cluster one group is dominated by HFSE (U, Pb, Th, Zr, Ta Y, Hf and Nb), minor presence of REEs (La and Ce), transition metals (Zn

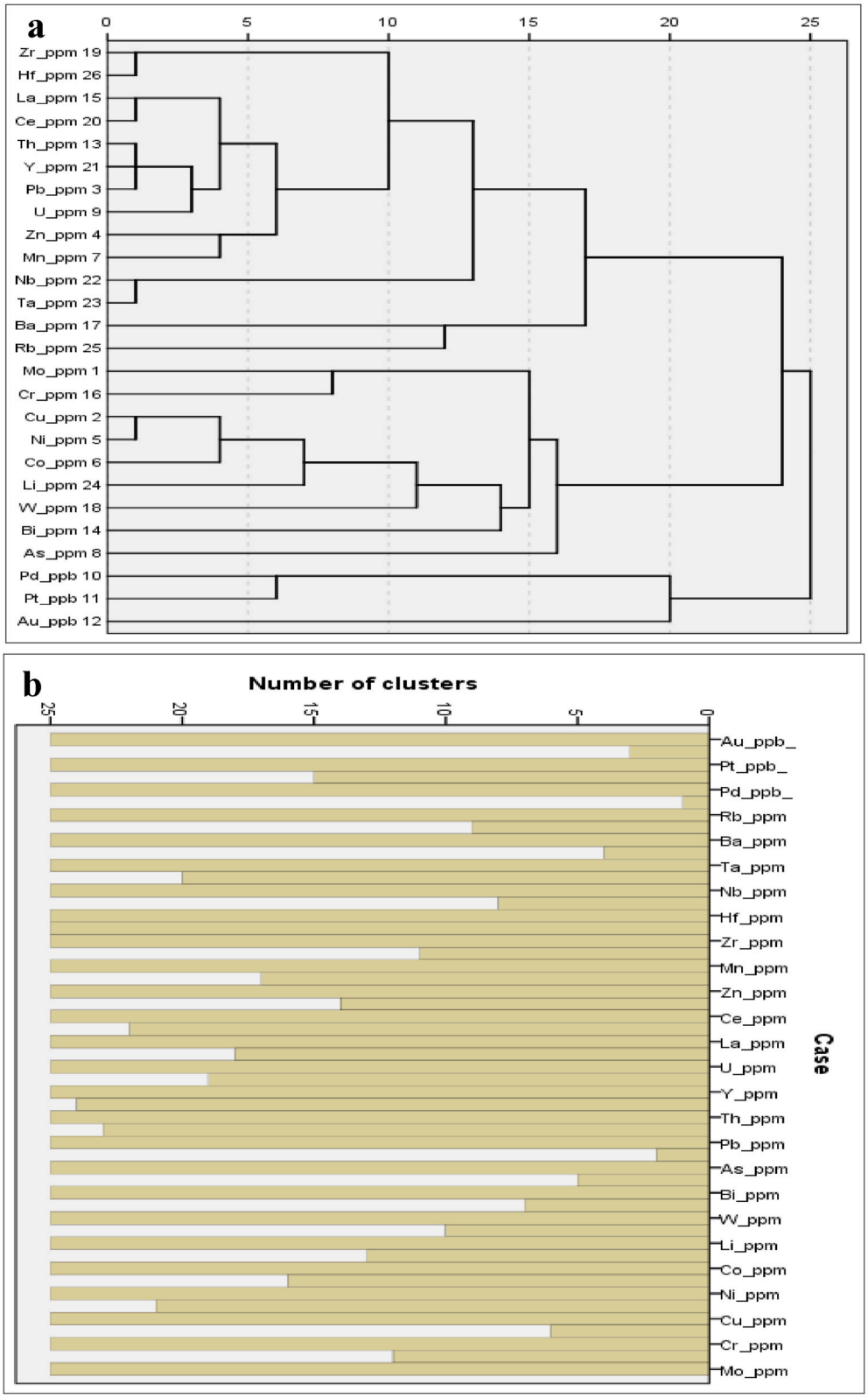

Fig. 5. Cluster analysis of data set presented by (a) dendrogram showing three sub classes marked by the phenon line and (b) a case-based clusters that shows the extent of similarity by bar between the measured elements.

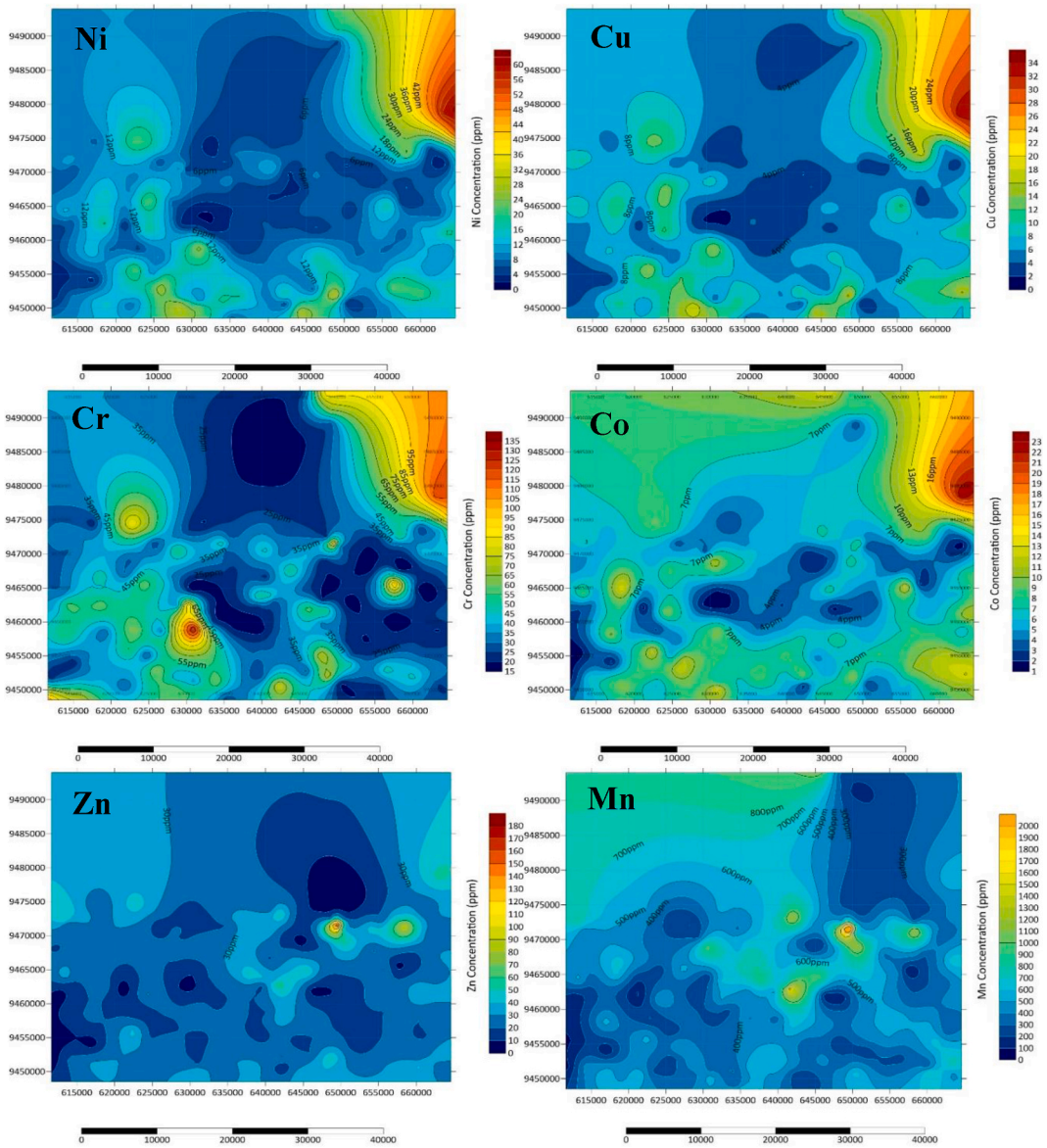

Fig. 6. Geospatial distribution of transition metals showing a much coherent pattern for Ni, Cu, Cr and Co, and a minor variability between Zn and Mn.

and Mo), and LILE (Ba and Rb). It is well established that HFSE and REEs tend to be concentrated in felsic rocks (continental crust). The concentrations of HFSE are controlled by the presence of certain mineral phases. For instance, concentration of the mineral zircon controls the concentration of Zr and Hf, and minerals of ilmenite, rutile and titanite controlling Th, Ta and REEs content. The underlying geology of the area is granitoid dominated (Fig. 1), and likely account for the HFSE and REE enrichment and contribution. Zn and Mo in cluster one likely suggests a source from mafic rocks or ferromagnesian mineral phases [53]. The LILE of Rb and Ba widely distributed in the area, and in cluster one could suggested a metasomatic alteration, especially associated with feldspar component largely in granitoids or plagioclase and/or carbonate minerals [38,54].

The Cluster 2 contains Mo, Cu, Ni, Co, As, Bi, Cr, W and Li, and cluster 3 with association of Pt, Pd and Au. Transition metal (Mo, Ni, Co, Cu and Cr) and other metals (Bi, Li and W) are often rich in mafic-ultramafic rocks [55,56] or enriched in the carbonaceous-rich shales as such are easily absorbed unto organic matter during sedimentation in anoxic environment [5]. As and Au enrichment could be related to the sulphide minerals (e.g., arsenopyrite, pyrite). But no correlation between Au and As (Table 2) could indicate likely differing sources. The behaving of Pb, Zn, Cu, As and Mo associated felsic volcanic rocks or partitioning into ferromagnesian minerals of biotite and amphiboles have been recognized [53]. Thus, the cluster 2 elements, and metals of Zn, Mn of cluster one is either source from mafic rocks or mafic minerals within the granitoids or both.

In addition to deciphering the likely source rock or mineral contributions to the obtained clusters, the geology of the terrane

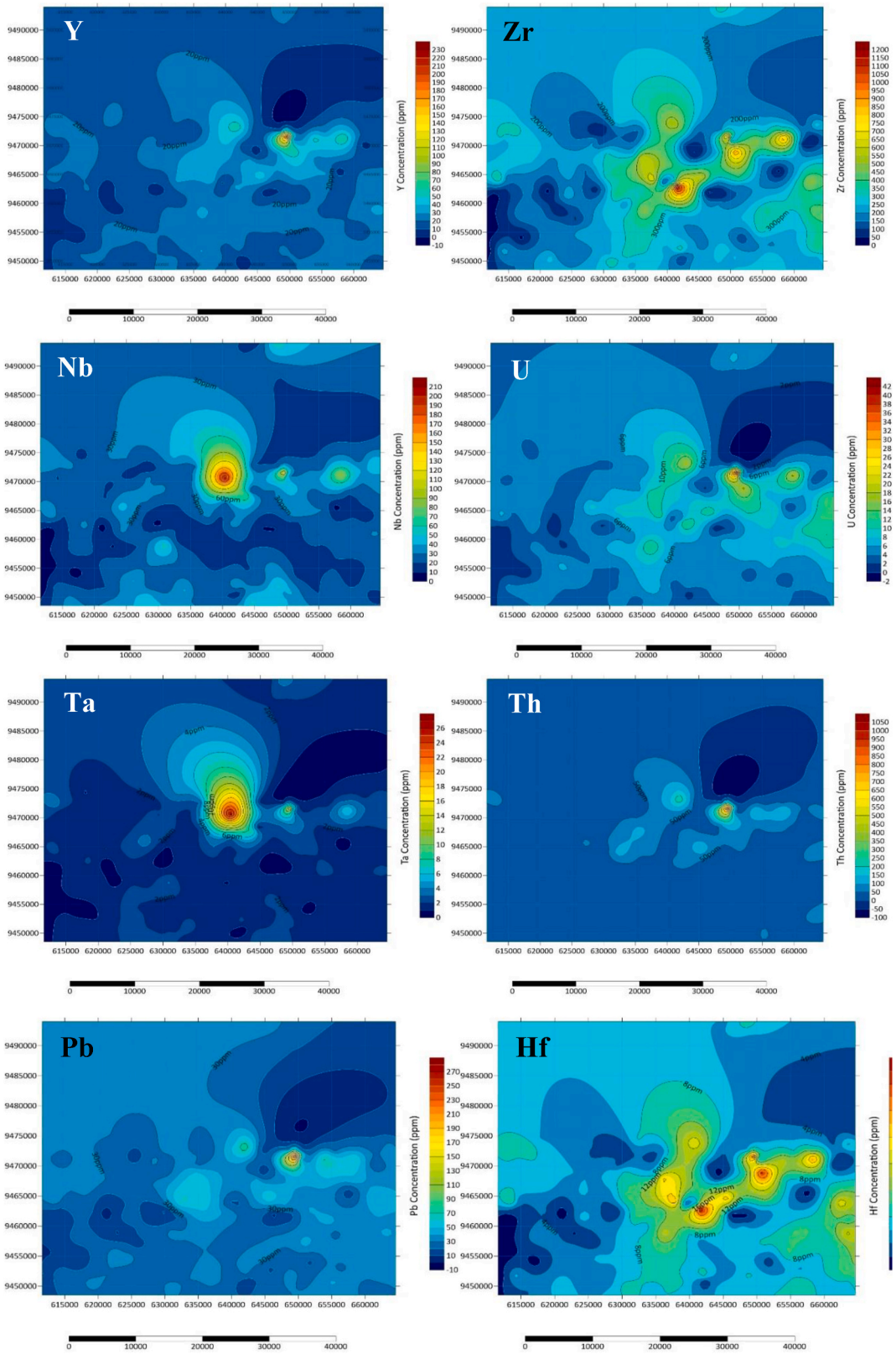

Fig. 7. Geospatial distribution of High Field Strength Elements showing general occurrence within the central domain of the area, except Zr, U and Hf that show much similar trend and a broader distribution towards the SE part of the area.

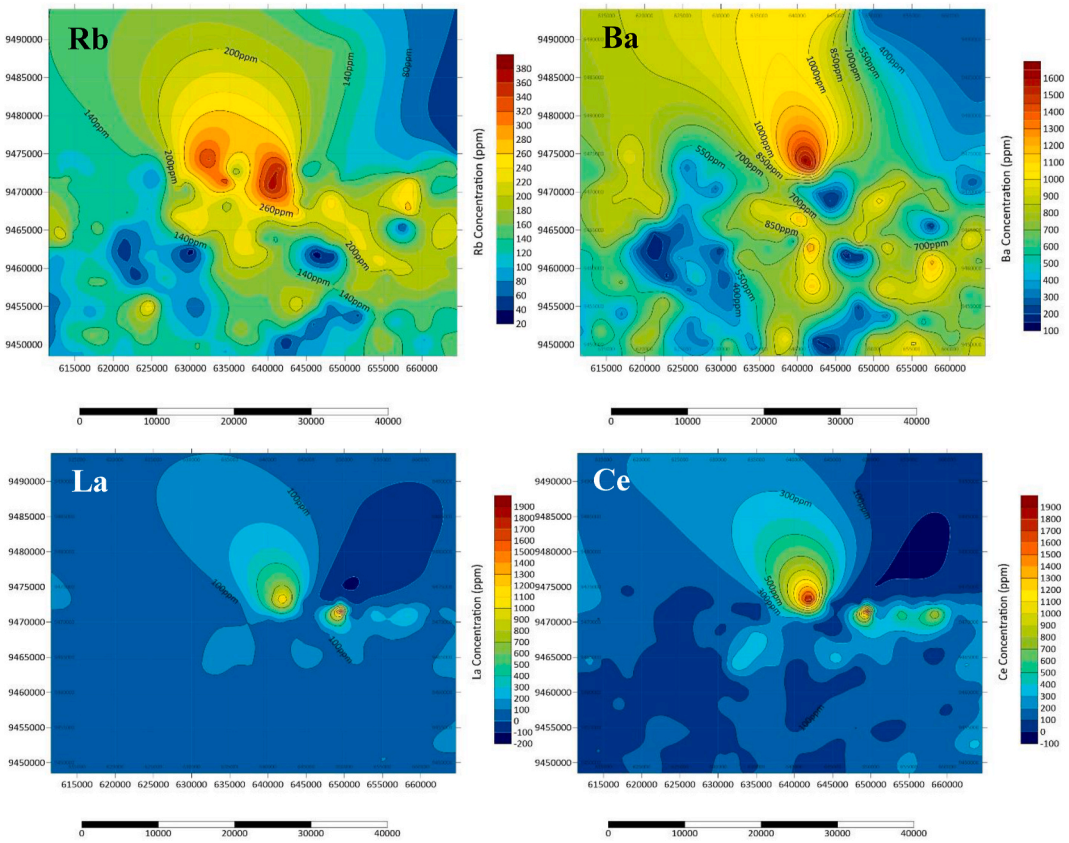

Fig. 8. Geospatial distribution of LILE showing a much coherent pattern for Rb and Ba, and for REEs with same pattern for between La and Ce.

possible control to a greater extent the input to the observed elemental distribution. Maximum contribution from the granitoid-migmatite rocks is envisage, and input from basalts, and fine-grained clastic sediment a likely support. According to Refs. [57–59] major and trace elements are a composite of mafic–ultramafic and felsic source proxies for clastic sediments. The analyzed stream sediments may be a reflection of a mixed sources but felsic rocks possible are promising source of anomalous elements observed.

6. Conclusion

A combined data processing approach of descriptive statistics, enrichment-depletion, data normalization, geospatial elemental distribution, and stacked overlayed comparison of elements have been used in this study. The following deduction are drawn.

1. Potential elements that need a follow-up exploration campaign as revealed from the cluster analysis are; Pb, Zn, Mn, U, Th, La, Zr, Ce, Y, Nb, Ta, Hf, Ba, Rb, Mo, Cu, Ni, Co, As, Bi, Cr, W, Li, Pt, Pd, and Au.
2. A poly-metallic source and processes controlled by the underlain geology are the most plausible drivers to the element distribution. Granitization is the major controlling factor, and represent possible source of HFSE and REEs, other metals may either be sourced from the mafic minerals associated with granitoids or other rocks of the terrane (fine clastic sedimentary rocks, and minor volcanic).
3. The adopted geostatistical methods and other approach utilized in this research are indicative of effective handling of bulk exploration data for further exploration decision making.

Data availability statement

Data will be made available upon request.

CRediT authorship contribution statement

Samuel Nunoo: Writing – review & editing, Writing – original draft, Validation, Formal analysis, Data curation, Conceptualization. **Benatus Norbert Mvile:** Writing – review & editing, Visualization, Resources, Methodology, Formal analysis, Conceptualization.

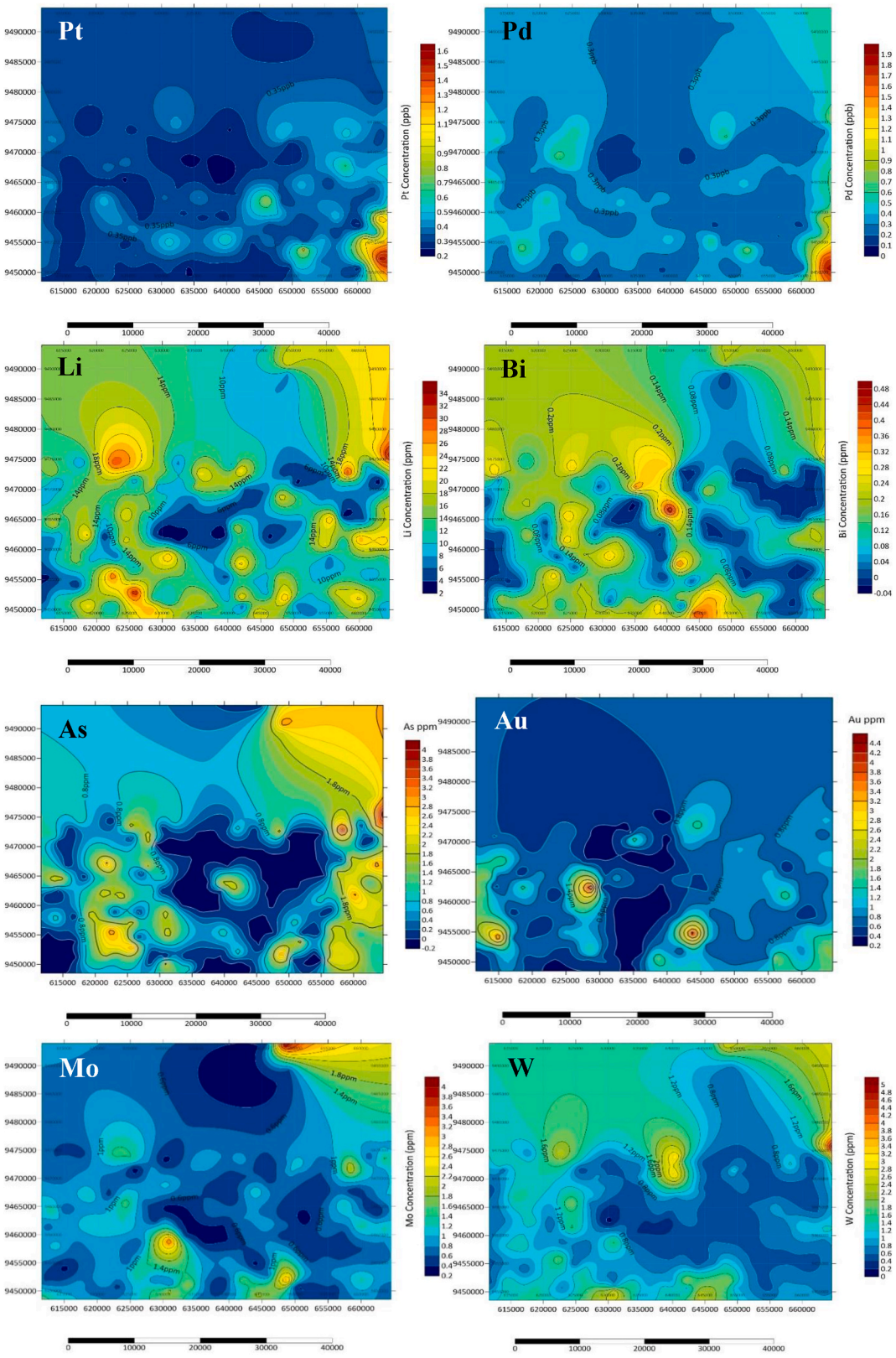

Fig. 9. Geospatial distribution of PGE (Pt and Pd) and Other Elements (Li, Bi, Au, As, Mo and W). Pt and Pd show similar pattern especially at the SE section, Li and Bi pattern are almost the same, remaining elements (Au, As, Mo and W) show variable distribution pattern.

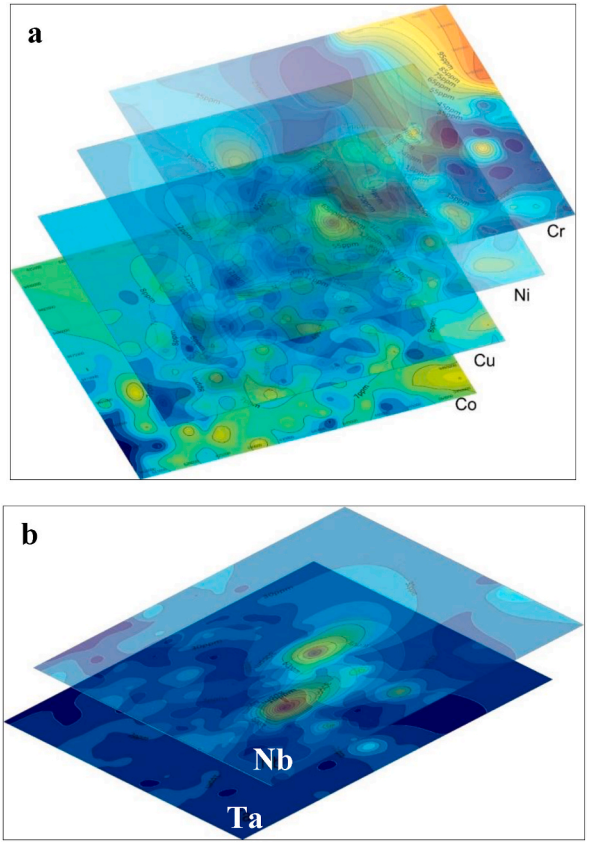

Fig. 10. Layered representation of selected elements (a &b) showing a compared similar geospatial element distribution.

Mahamuda Abu: Writing – review & editing, Writing – original draft, Visualization, Validation, Investigation, Formal analysis, Data curation, Conceptualization. **John Desderius Kelimenze:** Writing – review & editing, Validation, Software, Resources, Project administration, Methodology, Investigation, Conceptualization.

Declaration of competing interest

The authors declare that they have no known competing financial interests or personal relationships that could have appeared to influence the work reported in this paper.

Acknowledgement

The authors are thankful to the Geological Survey of Tanzania (GST) for providing all data used in this work.

References

[1] A.C. Colvine, A.J. Andrews, M.E. Cherry, M.E. Durocher, A.J. Fyon, M.J. Lavigne, A.J. MacDonald, S. Marmont, K.H. Poulsen, J.S. Springer, D.G. Troop, An integrated model for the origin of Archean lode gold deposis. Open File Report, Ontario Geological Survey p 5524 (1984).
[2] B.E. Nesbitt, J.B. Murrowchick, K. Muehlenbachs, Dual origin of lode gold deposits in the Canadian Cordillera, Geology 14 (1986) 506–509.
[3] H.W. Nesbitt, G.M. Young, Formation and diagenesis of weathering profiles, J. Geol. 97 (1989) 129–147.
[4] R.J. Goldfarb, T. Baker, B. Dube, D.I. Groves, C.J.R. Hart, P. Gosselin, Distribution, character, and genesis of gold deposits in metamorphic terrains, in: J. W. Hedenquist, J.F.H. Thompson, R.J. Goldfarb, J.P. Richards (Eds.), Econ. Geol. 100th Anniversary Volume 1905–2005: Littleton, Colorado, vol. 407, Society of Economic Geology, 2005, p. 450.
[5] R.R. Large, V. Maslennikov, F. Robert, L.V. Danyushevsky, Z. Chang, Multistage sedimentary and metamorphic origin of pyrite and gold in the giant Sukhoi Log deposit, Lena gold province, Russia, Econ. Geol. 102 (2007) 1232–1267.
[6] R.R. Large, S.W. Bull, V. Maslennikov, A carbonaceous sedimentary source-rock model for Carlin-type and orogenic gold deposits, Economic Geology and the Bulletin of the Society of Economic Geologist 106 (2011) 331–358.
[7] I.K. Pitcairn, D. Craw, D.A.H. Teagle, The gold conveyor belt: large-scale gold mobility in an active orogen, Ore Geol. Rev. 62 (2014) 129–142.
[8] A. Agangi, S.M. Reddy, D. Plavsa, C. Vieru, V. Selvaraja, C. LaFlamme, H. Jeon, L. Martin, T. Nozaki, Y. Takaya, K. Suzuki, Subsurface deposition of Cu-rich massive sulphide underneath a Palaeoproterozoic seafloor hydrothermal system—the Red Bore prospect, Western Australia, Miner. Deposita 53 (2018) 1061–1078.

[9] W.G. Garlick, Genetic interpretation from ore relations to algal reefs in Zambia and Zaire, in: R.W. Boyle, A.C. Brown, C.W. Jefferson, E.C. Jowett, R.V. Kirkham (Eds.), Sediment-hosted Stratiform Copper Deposits, vol. 36, Geological Association of Canada, Special Paper, 1989, pp. 471–498.
[10] P. Bartholomé, P. Evrard, F. Katekesha, J. Lopez-Ruiz, M. Ngongo, Diagenetic ore forming processes at kamoto, Katanga, republic of the Congo, in: G.C. Amstutz, A.J. Bernard (Eds.), Ores in Sediments, Springer-Verlag, Heidelberg, 1972, pp. 21–41.
[11] R.R. McGowan, S. Roberts, R.P. Foster, A.J. Boyce, D. Coller, Origin of the copper-cobalt deposits of the Zambian Copperbelt: an epigenetic view from Nchanga, Geology 31 (2003) 494–500.
[12] D. Selley, D. Broughton, R. Scott, M. Hitzman, S. Bull, R. Large, P. McGoldrick, M. Croaker, & N. Pollington, F. Barra, A New Look at the Geology of the Zambian Copperbelt. Society of Economic Geologists, 100th Anniversary, vols. 965–1000, 2005.
[13] H.A. El Desouky, Ph Muchez, A.J. Boyce, K. Schneider, J.L.H. Cailteux, S. Dewaele, A. von Quadt, Genesis of sedimenthosted stratiform copper-cobalt mineralization at luiswishi and kamoto, Katanga copperbelt (democratic republic of Congo), Miner. Deposita 45 (2010) 735–763.
[14] M. Haest, Ph Muchez, Stratiform and vein-type deposits in the Pan-African orogen in central and southern Africa: evidence for multiphase mineralisation, Geol. Belg. 14 (2011) 23–44.
[15] I.K. Pitcairn, D.A.H. Teagle, D. Craw, G.R. Olivo, R. Kerrich, T.S. Brewer, Sources of metals in orogenic gold deposits: insights from the Otago and Alpine Schists, New Zealand, Econ. Geol. 101 (2006) 1525–1546.
[16] D.I. Groves, R.J. Goldfarb, M. Gebre-Mariam, F. Robert, Orogenic gold deposits: a proposed classification in the context of their crustal distribution and relationship to other gold deposit types, Ore Geol. Rev. 13 (1998) 7–27.
[17] A.G. Tomkins, Windows of metamorphic sulfur liberation in the crust: implications for gold deposit genesis, Geochem. Cosmochim. Acta 74 (2010) 3246–3259.
[18] J.M.A. Hronsky, D.I. Groves, R.R. Loucks, G.C. Begg, A unified model for gold mineralisation in accretionary orogens and implications for regional-scale exploration targeting methods, Miner. Deposita 47 (2012) 339–358.
[19] E.M. Cameron, Archean gold: relation to granulite formation and redox zoning in the crust, Geology 16 (1988) 109–112.
[20] J.A. Fyon, D.G. Troop, S. Marmon, A.J. MacDonald, Introduction of gold into Archean crust, Superior Province, Ontario — coupling between mantle-initiated magmatism and lower crustal thermal maturation, Econ. Geol. Monogr. 6 (1989) 479–490.
[21] P.M. Nude, J.M. Asigri, S.M. Yidana, E. Arhin, G. Foli, J.M. Kutu, Identifying pathfinder elements for gold in multi-element soil geochemical data from the Wa-Lawra belt, northwest Ghana: a multivariate statistical approach, Int. J. Geosci. 3 (1) (2012) 62.
[22] B.N. Mvile, M. Abu, J. Kalimenze, Trace elements geochemistry of in situ regolith materials and their implication on gold mineralization and exploration targeting, Dodoma Region, East Africa, Mining, Metallurgy & Exploration 38 (5) (2021) 2075–2087.
[23] J.D. Kalimenze, M. Abu, B.N. Mvile, Soil geochemistry and multivariate statistical assessment of copper–gold-PGEs mineralization in parts of singida region of the Tanzania craton, Tanzania, East Africa, Arabian J. Geosci. 16 (2023) 59, https://doi.org/10.1007/s12517-022-11148-5.
[24] J.M. Kabete, D.I. Groves, N.J. McNaughton, A.H. Mruma, A new tectonic and temporal framework for the Tanzanian Shield: implications for gold metallogeny and undiscovered endowment, Ore Geol. Rev. 48 (2012) 88–124.
[25] G. Borg, R.M. Shackleton, The Tanzania and NE Zaire cratons, in: M. DeWit, L.D. Ashwal (Eds.), Greenstone Belts, Oxford University Press, Oxford, 1997, pp. 608–619.
[26] J.M. Kabete, D.I. Groves, N.J. McNaughton, A.H. Mruma, A new tectonic and temporal framework for the Tanzanian Shield: implications for gold metallogeny and undiscovered endowment, Ore Geol. Rev. 48 (2012) 88, 124et al., 2012.
[27] Y.A. Cook, I.V. Sanislav, J. Hammerli, T.G. Blenkinsop, P.H.G. Dirks, A primitive mantle source for the Neoarchean mafic rocks from the Tanzania Craton, Geosci. Front. 7 (2015) 911–926.
[28] S.D. Kwelwa, P.H. Dirks, I.V. Sanislav, T. Blenkinsop, S.L. Kolling, Archaean gold mineralization in an extensional setting: the structural history of the kukuluma and matandani deposits, geita greenstone belt, Tanzania, Minerals 8 (4) (2018) 171.
[29] J. Henckel, K.H. Poulsen, T. Sharp, P. Spora, Lake victoria goldfields, Episodes Journal of International Geoscience 39 (2) (2016) 135–154.
[30] C.M. Chamberlain, R.M. Tosdal, U–Pb Geochronology of the Lake Victoria Greenstone Terrane, Tanzania. Mineral Deposit Research Unit the University of British Columbia (Research Program on World-Class Gold Deposits and Advanced Exploration Projects Owned And/or Joint Ventured to Barrick Gold, Placer Dome, Anglogold-Ashanti, Resolute Mining NL as Main Sponsors, 2007.
[31] B. Yuksel, E. Arica, Assessment of toxic, essential, and other metal levels by ICP MS in lake eymir and mogan in ankara, Turkey: an environmental application, Atom. Spectros 39 (5) (2018).
[32] J.J. Egozcue, V. Pawlowsky-Glahn, G. Mateu-Figueras, C. Barcelo-Vidal, Isometric log ratio transformations for compositional data analysis, Math. Geol. 35 (3) (2003) 279 330.
[33] E.D. Sunkari, M. Appiah-Twum, A. Lermi, Spatial distribution and trace element geochemistry of laterites in Kunche area: implication for gold exploration targets in NW, Ghana, J. Afr. Earth Sci. 158 (2019), 103519.
[34] P. Goovaerts, Kriging interpolation, in: John P. Wilson (Ed.), The Geographic Information Science & Technology Body of Knowledge, 4th Quarter 2019 Edition, 2019, https://doi.org/10.22224/gistbok/2019.4.4.
[35] S.M. McLennan, Relationships between the Trace Element Compositions of Sedimentary Rocks and Upper Continental Crust. Geochemistry, Geophysics, Geosystems, 2001, 10. 1029/2000G C0001 09.
[36] B.E. Nesbitt, J.B. Murrowchick, K. Muehlenbachs, Dual origin of lode gold deposits in the Canadian Cordillera, Geology 14 (1986) 506–509.
[37] H.W. Nesbitt, G.M. Young, Formation and diagenesis of weathering profiles, J. Geol. 97 (1989) 129–147.
[38] C.M. Fedo, K.A. Eriksson, E.J. Krogstad, Geochemistry of shales from the archean (3.0 Ga) buhwa greenstone belt, Zimbabwe: Implications for provenance and source area weathering. Geochimica Cosmochimica Acta 60 (1996) 1751–1763.
[39] A. Moraga, G. Chong, M.A. Fortt, H. Henriquez, Estudio geolo'gico del salar de Atacama, Provincia de Antofagasta, vol. 29, Boleti´n del Instituto de Investigaciones Geolo´gicas, 1974, pp. 1–56.
[40] T. Boschetti, G. Cortecci, M. Barbieri, M. Mussi, New and past geochemical data on fresh to brine waters of the Salar de Atacama and Andean Altiplano, northern Chile, Geofluids 7 (2007) 33–50.
[41] J. Cabello, Lithium brine production, reserves, resources and exploration in Chile: an updated review, Ore Geol. Rev. 128 (2021), 103883.
[42] G. Kesse, The Mineral and Rocks Resources of Ghana, A.A. Balkema, Rotterdam, Boston, 1985, p. 609.
[43] J.P. Mile´si, P. Ledru, P. Ankrah, V. Johan, E. Marcoux, Ch Vinchon, The metallogenic relationship between Birimian and Tarkwaian gold deposits in Ghana, Miner. Deposits 26 (1991) 228–238.
[44] W. Hirdes, B. Nunoo, The Proterozoic Palaeoplacers at Tarkwa gold mine/SW Ghana. Sedimentology, mineralogy, and Precise age dating of the main Reef and West Reef, and bearing of the investigations on source area aspects, D 100, Geol. Jahrb. (1994) 247–311.
[45] J.-P. Pigois, D.I. Groves, I.R. Fletcher, N.J. McNaughton, L.W. Snee, Age constraints on Tarkwaian palaeoplacer and lode-gold formation in the Tarkwa-Damang district, SW Ghana, Miner. Deposita 38 (2003) 695–714.
[46] F. Atanga, P.O. Amponsah, S. Nunoo, D. Kwayisi, E.D. Forson, T.M. Akabzaa, P.M. Nude, The geology and geochemistry of the Rhyacian Josephine gold deposit, Northwest Ghana, B. Appl. Earth Sci. (2023), https://doi.org/10.1080/25726838.2023.2260583.
[47] C.A. Tarnocai, K. Hattori, L.J. Cabri, "Invisible" gold in sulfides from Campbell mine, Red lake greenstone belt, Ontario: evidence for mineralization during the peak of metamorphism, Can. Mineral. 35 (1997) 805–815.
[48] L.J. Cabri, M. Newville, R.A. Gordon, Chemical speciation of gold in arsenopyrite, Can. Mineral. 38 (2000) 1265–1281.
[49] M. Abu, S. Nunoo, W.R. Kazapoe, Geochemical and multivariate statistical characterization of shales of the Oti−Pendjari Group of the Neoproterozoic Basin of Ghana: implication of paleoweathering, climatic conditions, and provenance, Journal of Sedimentary Environments (2023), https://doi.org/10.1007/s43217-023-00125-x.
[50] R.C. Stanley, On the special application of Thompson–Howarth error analysis to geochemical variables exhibiting a nugget effect, Geochem. Explor. Environ. Anal. 6 (2006) 357–368.

[51] M. Abzalov, Quality control of assay data: a review of procedures for measuring and monitoring precision and accuracy, Explor. Min. Geol. 17 (3–4) (2008) 131–144, 2008.
[52] S.M. McLennan, S. Hemming, D.K. McDaniel, G.N. Hanson, Geochemical Approaches to Sedimentation, Provenance and Tectonics, vol. 284, Geological Society of America Special Paper, 1993, pp. 21–40.
[53] E.R. Johnson, V.S. Kamenetsky, J. McPhie, The behavior of metals (Pb, Zn, as, Mo, Cu) during crystallization and degassing of rhyolites from the okataina volcanic center, taupo volcanic zone, New Zealand, J. Petrol. 54 (8) (2013) 1641–1659.
[54] C.M. Fedo, H.W. Nesbitt, G.M. Young, Unraveling the effects of potassium metasomatism in sedimentary rocks and paleosols, with implications for paleoweathering conditions and provenance, Geology 23 (1995) 921–924.
[55] S.M. Jowitt, G.R.T. Jenkin, L.A. Coogan, J. Naden, Quantifying the release of base metals from source rocks for volcanogenic massive sulfide deposits: effects of protolith composition and alteration mineralogy, J. Geochem. Explor. 118 (2012) 47–59.
[56] C.J.L. Wilson, P. Schaubs, L.D. Leader, Mineral Precipitation in the Quartz Reefs of the Bendigo Gold Deposit, vol. 108, Economic Geology and the Bulletin of the Society of Economic Geologist, Victoria, Australia, 2013, pp. 259–278.
[57] R.L. Cullers, T. Barrett, R. Carlson, B. Robinson, Rare earth element and mineralogic changes in Holocene soil and stream sediment: a case study in the wet mountains region, Colorado, USA, Chem. Geol. 63 (1987) 275–297.
[58] R.L. Cullers, A. Basu, L. Suttner, Geochemical signature of provenance in sand size material in soils and stream sediments near the Tobacco Root batholith, Montana, USA, Chem. Geol. 70 (4) (1988) 335–348.
[59] S.R. Taylor, S.M. McLennan, The Continental Crust: its Composition and Evolution, Blackwell, Oxford, 1985.